Proceedings of the
International Conference on Mechanical Engineering 2009
(ICME2009) 26- 28 December 2009, Dhaka, Bangladesh

ICME09-FM-21

REDISTRIBUTED GAS EXCHANGE MECHANISM IN HUMAN LUNG'S PERIPHERALS

M. U. Ahmmed, H. Hirahara and T. Yamamoto

Graduate School of Science and Engineering,
Saitama University, Shimo-Okubo, Sakura, Saitama,338-8570, Japan

ABSTRACT

The velocity distribution was investigated with particle image velocimetry (PIV) in a real size model of human's lung peripherals. The working gas is air and the oil mist was used as a tracer. The unsteady velocity profile was obtained with phase locked image capturing, and the data was processed in statistically. The target region of this study is between the 18th to 20th bifurcations in lung's airway. The fundamental respiratory flow was investigated in the present experiment under the high frequency oscillatory ventilation (HFOV) mode for the different compliance conditions, which is important for the clinical treatment. According to the mean flow analysis, the phase delay was estimated theoretically and obtained experimentally. The phase delay in the mean flow was very small, however the obvious flow mixing was observed in the air path lines.

Keywords: Human lung, PIV, Compliance, HFOV, Redistribution of Gas.

1. INTRODUCTION

A Gas flow in the mammal lungs is simply reciprocal, however, the efficient gas exchange was carried out through this simple air motion. In order to establish the effective gas exchange between oxygen and carbon dioxide, the mammals have developed the sophisticated mechanism in a process of evolution. The gas flow in lungs is so complicated that the flow mechanism has not yet been cleared in the view of the micro or molecular scale. The damage of lung's function arise the critical situation to the human. For these treatments, a lot of effective artificial ventilation devices have been proposed for the lung diseases. HFOV is one of the effective devices for this treatment.

The aim of the present study is to analyze the air trajectory and gas mixing process in the peripherals of lung under the HFOV condition. The fresh air distribution in the bronchial tree is a very important factor in the gas exchange controls of lungs. The heterogeneous compliance distribution will form a different response in the periodic flow motion, thus the time constant in the unsteady flow is different in each branch.

In the present paper, the delay time was compared to the theoretical prediction of electric circuit similarity analysis. The fresh air distribution is associated with the complex flow pattern due to the asymmetric bronchial configuration. In medical treatment, HFOV has a advantage for the minimal pressure fluctuations with a small tidal volume which can avoid the risk of lung injury associated with cyclic opening and closing of alveolar units, especially for very early born infants who are suffered with respiratory distress syndrome (RDS). Since the tidal volume in HFOV is usually much smaller than the anatomical dead space volume, the prompt gas exchange shown in this operation cannot be explained in terms of simple advective bulk transport to the alveoli. The air transport mechanism has not been cleared, the more detailed fluid dynamical research for HFOV system will be desired to develop the clinical treatment under the optimum condition.

According to the previous researches, it was found that the gas exchange efficiency depends on the Taylor's dispersion, pendelluft and molecular diffusion etc. The fundamental mechanism of pendelluft is attributed to the difference of time constant between lung units due to airway resistance and compliance. In HFOV, it is expected that pendelluft plays an important role on gas exchange; however, all mechanisms of gas transport and exchange have not been yet clarified in detail.

Asymmetry and irregularity of the peripherals has the significant roles in the gas mixing and exchange mechanism. In order to investigate the flow mixing mechanism in the gas exchange zone, many studies have been carried out by considering the human airway models. Otis et al. [1] predicted that asynchronous fluid flow with associated inter-regional convection between parallel respiratory units can result from non-homogeneities in tissue mechanics, and such flows are known as 'pendelluft' flows which are now regarded as an important factor in gas mixing during high frequency ventilation [2]. Ultman et al. [3] and High et al. [4] carried out a study of pendelluft and mixing in a

single bifurcation lung model during HFOV. They obtained the mixing coefficients and the pendelluft volume fraction. They also show that asymmetries in compliance and in inertance produce much greater pendelluft than an asymmetry in resistance. Elad et al.[5] developed a nonlinear lumped-parameter model to investigate the dependency of airflow distribution in asymmetric bronchial bifurcations on structural and physiological parameters. They derived the modified time-dependent expressions of resistance and compliance of each compartment. They also showed that asymmetry in compliance of peripheral airways might affect the flow distribution in daughter tubes and induced larger degrees of pendelluft.

To facilitate investigation of gas mixing and exchange in bronchial tube, efforts have been directed towards the development of air path trajectory. The ensemble mean velocity vectors were obtained through the experiment. The Lagrangian path line of air from the time mean velocity distribution data was reconstructed.

2. PULMONARY PHYSIOLOGY AND ANALOGY

2.1 Anatomical Background

The air way of human lung is divided into 23 generations. These airways consist of successive two zones, conducting zone and the respiratory zone. From trachea to the bronchioles (G0 to G16, where G is generation), no alveoli exits and no gas exchange occurs so that this space is called anatomical dead space. Down to the conducting zone the respiratory zone (G17 to G23) starts and continues to respiratory bronchioles, alveolar ducts and alveolar sacs. In this region a vast number of alveoli exist and hence suitable gas exchange occurs.

Gas diffusion is dominated in the bottom of the lung, whereas, in the respiratory region an active gas mixing will be expected to maintain the effective molecular diffusion. The end part of lung in which the inhaled air contacts with the residual air, has complicated bronchial tissue with bifurcated micro-channels where the complicated gas exchange mechanism occurs by not only molecular diffusion but also convective motion.

Oscillatory air flow generated by artificial ventilation system HFOV is an important process to develop the rate of gas exchange in deeper branches of bronchial tube. The oscillatory flow exhibits an important characteristic length as Stokes layer thickness, $\delta = \sqrt{\frac{2\nu}{\omega}}$, where ν (= 1.513 $\times 10^{-5}$ m^2/s, 20 degrees in Celsius for air) is the kinematic viscosity, ω ($= 2\pi f$, f is the frequency) is the angular frequency. Two fundamental dimensionless parameters for the oscillatory flow are Reynolds number and Womersley number. They are defined as $Re = ud/\nu$ and $\alpha = \frac{d/2}{\sqrt{\frac{\omega}{2\nu}}}$, respectively. Where, u and d are averaged flow speed and the diameter of channel respectively.

Under the normal breathing condition, Re is about 4000 at the trachea and about 30 at terminal bronchus where it is less than 0.04 in the alveolar region. Hence the average fluid velocity at the centre of the alveolar sac closes to zero so that the velocity in the alveoli is assumed to be slow streaming velocity. As described above, the flow features are very different in each generation. Furthermore, under HFOV driving condition, the flow regime should be changed drastically. In order to clarify the gas exchange mechanism both in the case of normal respiration and HFOV, the accurate flow measurement should be required. The frequency is 25~100 times of the normal breath for HFOV condition. Since α is proportional to the root of frequency, for large number of α, the phase delay is increased in velocity profiles between the main flow and the boundary layer. Consequently, the local disturbance will be induced near the brunches.

2.2 Lump Parameter Analysis

The air flow distribution in the bronchial tree is associated with the complex flow pattern and subjected to the nonlinear features of lung's mechanics. Direct in vivo study of airflow in lung is almost impossible and has been limited to evaluation of the frequency response of the respiratory system. The increasing of ventilation frequency or stroke volume increases the time and percentage of pendelluft in each cycle (Elad et al. [5]). Time constant difference or phase delay measurement between two sections of bronchial tube is another important assignment for better understanding of pendelluft motion. The generation of the pendelluft is predicted with the lump parameter analogy. The circuit of this analogy was demonstrated in Figure 1 for the present experiment.

The simulated synthetic impedance (Z_{19}) in the first junction may be expressed as

$$\begin{aligned} Z_{19} &= \frac{1}{(\sum R_i)^2 + (\sum S_i)^2}\left[\begin{array}{l}\left(R_1|Z_2|^2 + R_2|Z_1|^2\right) \\ + j\left(S_1|Z_2|^2 + S_2|Z_1|^2\right)\end{array}\right] \\ &= X_{19} + jY_{19} \\ &= \sqrt{X_{19}^2 + Y_{19}^2}\, e^{j\phi_{19}} \end{aligned} \quad (1)$$

$$where \quad \phi_{19} = \tan^{-1}\left(\frac{Y_{19}}{X_{19}}\right)$$

$$|Z_i|^2 = (X_{20i} + R_{19i})^2 + (Y_{20i} + S_{19i})^2$$

$$S_i = \omega L_i, \quad \text{for } G19$$

$$S_i = \omega L_i - \frac{1}{\omega C_i}, \quad \text{for } G20$$

$$i = 1\,(\text{for left branch}),\ 2\,(\text{for right branch}). \quad (2)$$

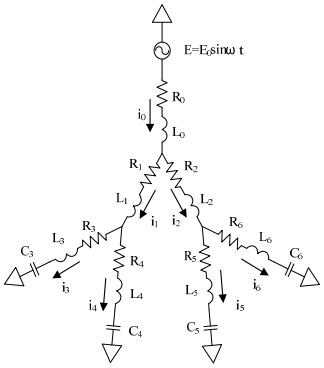

Fig 1. RLC circuit analogy

To simulate the present investigation, the resistive, inertial and elastic properties of the respiratory system have been replaced with RLC electrical circuits.
We adopted the empirical resistance law of Collins et al. [6] for each airway which is time-dependant and reflects the influence of curvature and the boundary layer development. This law is defined as in equation (3).

$$R = R_L\left(0.556 + 0.067\sqrt{Re}\right) \tag{3}$$

Here, $R_L = \frac{128\mu l}{\pi d^4}$ is the laminar flow resistance in a circular tube, l the length of the tube and μ the viscosity of the air.
In an oscillatory flow the pressure gradient that drives the fluid makes the inertia (acceleration and deceleration). The inertance corresponds to the fluid acceleration and can be expressed in terms of tube dimensions (Van der Tweel[7]), thus,

$$L = \frac{4\rho l}{\pi d^2}, \tag{4}$$

where ρ is the density of air. Since, air is practically incompressible within the real scale of bronchial tube, the inertance is independent of time.
In our experiment, the bronchial branches of G20 are connected to the rubber tubes which have the volume-dependant compliance, dV/dp of peripheral airways and lung tissue, whereas G18 and G1^h hold the constant volume as rigid tube made of metal plate and glass. According to the investigation of Sharp et al. [8], the net lung's compliance has a range in value

$$C_{Lung} = 0.125 \sim 0.31 \left[\frac{L}{cmH_2O}\right]$$

The compliance per unit lenght of rubber tube used in the experiment is

$$C_{Tube} = 7.88 \times 10^{-3} \left[\frac{\frac{ml}{cmH_2O}}{cm}\right] \tag{5}$$

The compliance below G20 was estimated from the number of the blanch and the length of the tube was adjusted for the equivalent compliance.
The combined resistance of bronchial model tube is simulated as

$$R_{combined} = R_{metal} + R_{glass} + R_{fitting} + R_{rubber\ tube} \tag{6}$$

The combined results for *Re* and *L* are also obtained by employing the equation (6).
The impedance of G19depends on the real resistance and inertance only. So, the local pendelluft in the first junction is generated by the influence of inertance which may induce the lateral mixing of air particles.

3. EXPERIMENTAL METHOD AND SETUP

3.1 Bronchial Model

In order to investigate the flow mechanism in lung, the instantaneous velocity vector fields are obtained for the different phase timing through the influx and efflux. By using these data, the periodic velocity distributions were obtained and fluid tracking was conducted for two cycles. According to the anatomical structure, a multi-bifurcated micro channel was used in the experiment as shown in Fig.2.
The test channels made of aluminum plate were pre-processed with black coating in order to reduce optical scattering. The channel widths of the G18, G19, and G20 generations were 500μm, 450μm and 400μm respectively as shown in Fig.2. The depth of each channel was 500μm.
The length of the G19 was 1.2mm along the centre line. The angles of first and second junction were 70 and 60 degrees respectively.

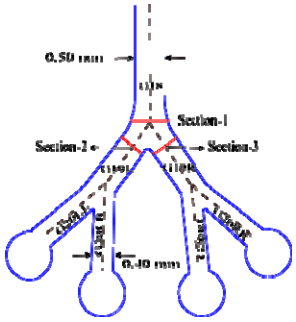

Fig 2. Bronchial model tube

Each branch of G20 was terminated with closed flexible tube which represents the peripheral alveoli. The tube is TYGON R-3603 (SAINT-GOBAIN Co'LTD).. The standard compliance of human under G20 is $2.0 \times \frac{10^{-2} ml}{cmH_2O}$. Hereafter, we call this compliance as 1-unit standard compliance. By changing its length, we can obtain the desired compliance to match the standard human lung. The driving system of HFOV was connected to a chamber. The chamber was connected to the test section and served a premixed mixture of air and tracer particles. The tidal volume and the amplitude of pressure variation were controlled by the controller of HFOV system.

3.2 Experimental Apparatus

Fig.3 shows schematic of the experimental setup for μ-PIV, which is consisted of ventilation system (HFOV),

test channel, image acquisition system, and illumination laser.

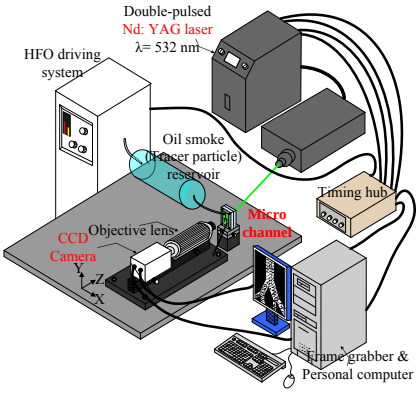

Fig.3 Schematic of experimental setup

The ventilation mode was generated by HFOV driver. The signals from pressure sensor were used for phase locking image acquisition.

The μ-PIV system for 2D velocity field measurements was consisted of high speed CMOS camera (IDT, XS-5), a macro lens with long working distance (KEYENCE, VQ-Z50A, ×500), double-pulsed Nd-YAG laser (New Wave Research, Solo III), timing hub, and computer for image capturing. The test section was illuminated by Nd-YAG laser with 532 nm wavelength, 50mJ/pulse output and 5ns duration from the backside of the micro channel at angle of 60 degree to prevent the damage of camera. The resolution of CMOS is 1280(H)×1024(V) pixels in space and 8 bits in depth of intensity. The maximum frame rate is 1000 frames per second. In our experiment, the oil-mist particles in the order of 1μm in diameter generated by Laskin nozzle were used as seeding particles. These particles are mixed in the premix chamber which connected to the inlet of the test channel.

4. RESULTS AND DISCUSSIONS

4.1 Instantaneous and Time Mean Velocity Distributions

The phase locked measurement was carried out in order to investigate the periodic oscillatory flow in multi-bifurcated airway models during HFOV condition at 10, 15, and 20 Hz. The phase locked signal was synchronized with the pressure signal and the delay time, $n\Delta T\ (n = 0,1,2,\ldots 15)$. Here, T is the period of oscillatory flow, and $\Delta T = \left(\frac{1}{16}\right)T$. 500 pair images were acquired for each delay time. The time mean velocity fields were obtained with these data. The size of the observation area was 2.8x2.3 mm, the image size recorded by micro-PIV system was 1280(H) ×1024(V) pixels and the interrogation window size for velocity reconstruction was 16x16 pixels.

Fig.2 shows the measurement sections of velocity profiles and Fig.4 exhibits the velocity profiles at sections 1, 2 and 3. The velocity profiles in the parent tube (Section-1) are approximately parabolic and oscillated in phase with driving force. If frequency increases, Womersley number also increases and a little unsteady nature of velocity profiles are observed in identical sections. As a result, we notice the asymmetric flow patterns in the daughter channels (Section-2, 3). This unsteadiness depends on time constant difference between parallel branches. In order to clarify the effect of phase delay we use two different volume ratios (4:4:4:4) and (4:4:1:1) and we perform our entire experiment by fixing a constant inspiration phase as a critical ventilation.

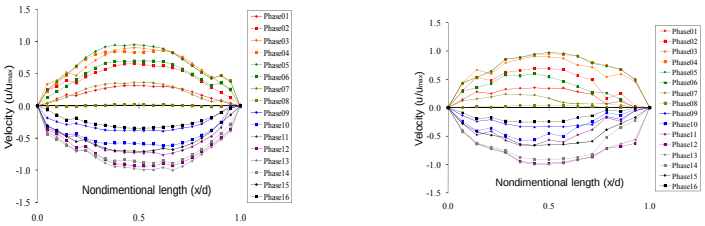

(a) Section-1 (b) Section-2

In case of even ratio (4:4:4:4), the vectors did not show symmetrical distribution. This was attributed to the difficulty of the fabrication of the model channels and the contamination of particle mist.

From Fig.4, if frequency are increased for symmetric volume ratio, the velocity profiles are about to parabolic. This happens for unsteadiness of flow and the phase delay occurs. This effect is noted in first junction of particle trajectory as shown in Fig.5. Also a very small pendelluft (small vortices) was observed in first junction, thus it is called a local stream. Moreover, this phase delay may occur by the combined effect of bifurcated junction, the oscillating viscous boundary layer and the tendency of lateral mixing. The phase delay is revealed from experimental results and RLC analogy model as shown in Table.1

Table: Comparison of phase delay

	Frequency	Volume ratio	Phase delay [ms] (Experiment)	Phase delay [ms] (RLC circuit)
Td02	10 Hz	4:4:4:4	5.95E-01	6.78E-01
		4:4:1:1	6.01E-01	6.77E-01
	15 Hz	4:4:4:4	6.10E-01	6.67E-01
		4:4:1:1	5.08E-01	6.68E-01
	20 Hz	4:4:4:4	7.25E-01	6.53E-01
		4:4:1:1	2.52E-01	6.46E-01

observed during an oscillatory flow through a Y-shaped tube bifurcation model. This is the effect of the

asymmetric geometry on the oscillating velocity vector field. It can be deduced that the quasi-steady redistribution is greatest for fluid elements that experience the highest velocity through the bifurcation junction. The redistributed field contributes to a complex

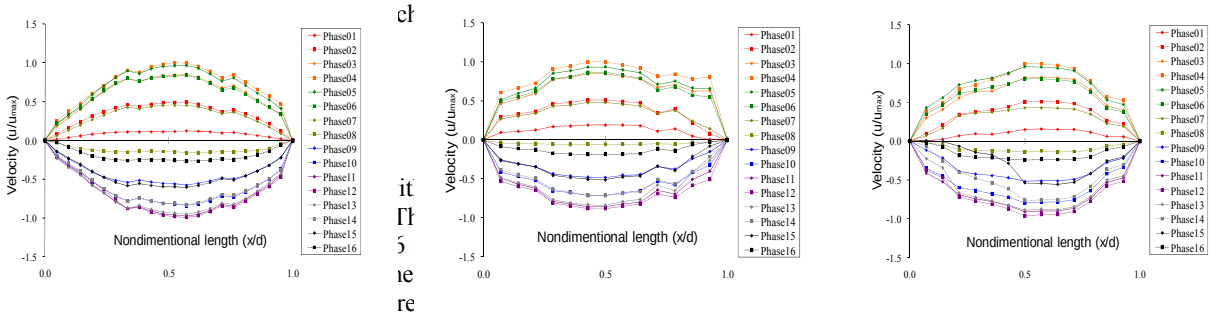

(d) Section-1 (e) Section-2 (f) Section-3

Fig.4 Velocity profiles at sections 1, 2 and 3 for 10 Hz (a, b, c) and 15 Hz (d, e, f)

vector maps of time interval $^1/_8\Delta T$ were obtained by interpolation of the experimental data.

Fig.5 shows, at the start of inspiration, 13 red markers were introduced in the parent channel (G18). For a complete cycle, the red dots for inspiration and the blue dots for expiration are air trajectory. For f=15 Hz and the volume ration (4:4:4:4), the path lines seem to be almost symmetric as shown in Fig. 5(a).

The obtained path lines are so complicated and interesting. The markers go down along the bifurcated channel in the inspiration phase and come back in the expiration phase. We see that the markers are deviated to the centre side and most of them over come the starting positions. The markers which were introduced inner side , they moved back by a little deviation and few of them could not reach the initial position. As mentioned here, this is an important mixing mechanism for this respiratory condition. During several cycles, the outer side air moves to the centre side and the centre side air moves to the deep location. Other words, the markers turn anticlockwise in left branch and clockwise in right branch. This mixing mechanism should be the most important reason on the redistribution of air. Fig. 5(b) shows that the compliance of left branch is four times larger than that of right branch by the conditions (4:4:1:1) and 15 Hz. So, flow rate becomes uneven for this asymmetric ratio and the markers of right branch show the quasi laminar behavior. Then, all markers returned to the starting position and exceeded their initial line.

By similar condition, if frequency is increased by 20 Hz , the path lines show the different features as shown in Fig.5(c). The markers of both branches penetrate to more deep location. The markers of right branch do not reach their starting position whereas almost all particles of left branch exceed their initial position. The small period for larger frequency and smaller flow rate does not effect on pendelluft but a very little time constant difference may induce a vortex generation which leads to the different path of the particles thus called redistribution.

5. CONCLUSION

Ensemble mean velocity distributions under the HFOV condition were obtained for a bronchial model tube for generation 18th to 20th of human lung with micro-PIV system. The phase delay was discussed for the different compliance and driving frequencies. The identical phase delay is observed from experiment and RLC analogy circuit model. By using the experimental velocity data, air trajectories were determined for several experimental conditions. We observe that oscillatory flow pattern changes for increasing of the driving frequency and for decreasing of Stoke's layer thickness.

The lines show the very complicated trajectories and these characteristic behaviors give a very important insight for the air redistribution in human airway of lung.

6. REFERENCES

1. Otis, A.B., McCarron, C.B., Bartlett, R.A., Mead, J., Mcilroy, M.B., Selverstone, N.J., and Radford, E.P., 1956,"Mechanical factors in distribution of pulmonary ventilation", Journal of Applied Physiology, 8: 427-443.
2. Chang, H.K.,1984, " Mechanisms of gas transport during ventilation by high-frequency oscillation", Journal of Applied Physiology, 56: 553-563.
3. Ultman, J. S., Shaw, R.G., Fabiano, D.C. and Cooke, K.A.,1988, "Pendelluft and mixing in a single bifurcation lung model during high frequency oscillation", Journal of Applied Physiology, 5:146-155 .
4. High K.C., Ultman J.S. and Karl S.R., 1991," Mechanically induced pendelluft flow in a model airway bifurcation during high frequency oscillation", Journal of Biomechanical Engineering, 113:342-347.
5. Elad, D., Shochat, A. and Shiner, R.J., 1998," Computational model of oscillatory airflow in a bronchial bifurcation", Respiration Physiology, 112:95-111.
6. Collins, J.M., Shapiro, A.H., Kimmel, E., Kamma, R.D., 1993, "The steady expiratory pressure-flow relation in a model pulmonary bifurcation", J. Biomech. Eng., 115:299-305.
7. Van der Tweel, L.H., 1957," Some physical aspects of blood pressure pulse wave, and blood pressure

measurements", Am. Heart J., 53:4-22.
8. Sharp , J.T., Henry, J.P., Sweany, S.K.,1964," The total work of breathing in normal and obese men", Journal of Clinical Investigation, 43:728-739.

7. NOMENCLATURE

Symbol	Meaning	Unit
G	Generation	
d	Diameter of each compartment	(mm)
f	Frequency	(Hz)
ω	Angular frequency	(rad /s)
ν	Kinematic viscocity	(m^2/s)
u	Average flow speed	(mm/s)
α	Womerseley number	(Dimensionless)
δ	Stokes layer thickness	(Dimensionless)
R_i	Resistance of each compartment	(ohms)
Z_i	Impedance of each compartment	(ohms)
S_i	Total reactance of each compartment	(ohms)
R	Airway resistance	($cmH_2O.L^{-1}.sec$)
R_L	Laminar resistance	($cmH_2O.L^{-1}.sec$)
ρ	Air density	(kg/m^3)
l	Tube length	(mm)
L	Inertance	($cmH_2O.L^{-1}.sec^2$)
φ	Phase delay	(sec)
C	Compliance	(L/cmH_2O)